



Mechanism of lateral ordering of InP dots grown on InGaP layers

J. R. R. Bortoleto, H. R. Gutiérrez, M. A. Cotta, and J. Bettini

Citation: *Applied Physics Letters* **87**, 013105 (2005); doi: 10.1063/1.1953875

View online: <http://dx.doi.org/10.1063/1.1953875>

View Table of Contents: <http://scitation.aip.org/content/aip/journal/apl/87/1?ver=pdfcov>

Published by the [AIP Publishing](#)

Articles you may be interested in

[Surface InP/In_{0.48}Ga_{0.52}P quantum dots: Carrier recombination dynamics and their interaction with fluorescent dyes](#)

J. Appl. Phys. **114**, 163510 (2013); 10.1063/1.4827188

[Localized growth of InAs quantum dots on nanopatterned InP\(001\) substrates](#)

Appl. Phys. Lett. **94**, 051109 (2009); 10.1063/1.3078275

[Relaxed, high-quality InP on GaAs by using InGaAs and InGaP graded buffers to avoid phase separation](#)

J. Appl. Phys. **102**, 033511 (2007); 10.1063/1.2764204

[Rapid thermal annealing of In As Ga As quantum dots with a low-temperature-grown InGaP cap layer](#)

J. Vac. Sci. Technol. A **24**, 700 (2006); 10.1116/1.2165655

[Radiative recombination from InP quantum dots on \(100\) GaP](#)

Appl. Phys. Lett. **78**, 2163 (2001); 10.1063/1.1361277



AIP | Journal of
Applied Physics

Journal of Applied Physics is pleased to
announce **André Anders** as its new Editor-in-Chief

Mechanism of lateral ordering of InP dots grown on InGaP layers

J. R. R. Bortoleto,^{a)} H. R. Gutiérrez,^{b)} and M. A. Cotta

Instituto de Física Gleb Wataghin, DFA, UNICAMP, CP 6165, 13081-970 Campinas-SP, Brazil

J. Bettini

Laboratório Nacional de Luz Sincrotron, CP 6192, 13084-971, Campinas-SP, Brazil

(Received 7 April 2005; accepted 17 May 2005; published online 28 June 2005)

The mechanisms leading to the spontaneous formation of a two-dimensional array of InP/InGaP dots grown by chemical-beam epitaxy are discussed. Samples where the InGaP buffer layer was grown at different conditions were characterized by transmission electron microscopy. Our results indicate that a periodic strain field related to lateral two-dimensional compositional modulation in the InGaP buffer layer determines the dot nucleation positions during InP growth. Although the periodic strain field in the InGaP is large enough to align the InP dots, both their shape and optical properties are effectively unaltered. This result shows that compositional modulation can be used as a tool for *in situ* dot positioning. © 2005 American Institute of Physics. [DOI: 10.1063/1.1953875]

Fabrication of nanoscale structures in the area of semiconductors has attracted considerable attention due to their potential application in novel devices based on a three-dimensional quantum confinement.¹ In particular, self-assembly of nanostructures via Stranski–Krastanow growth mode is a promising approach for high-throughput nanofabrication.² However, such nanostructures are usually randomly distributed over a planar substrate and fluctuate in size. This creates significant limitations for electronic device applications. Therefore, considerable effort has been focused on controlling the size, uniformity, density, and position of the self-assembling nanostructures.^{2–4} In a previous work, we reported the spontaneous formation of a two-dimensional array of self-organized InP/InGaP dots for In-rich coherent InGaP layers,⁵ which could be caused either by compositional modulation^{6–14} and/or atomic ordering¹⁵ phenomena present on our InGaP layers.

In this letter, we address the relevance of each of these mechanisms for InP dot nucleation on preferential sites. For this analysis, we have studied samples with InGaP buffer layers grown under different conditions (In content and V/III ratio). Structural characterization was carried out by transmission electron microscopy (TEM) and atomic force microscopy (AFM) measurements. Our results show no correlation between the InP dot positioning and the CuPt-type ordered domains of the InGaP layer. Samples with a higher lateral ordering degree exhibit a weaker atomic ordering phenomenon. In contrast, a strong correlation between the spatial distribution of InP dots and the compositional modulation inside the InGaP buffer layer is observed. In this way, the periodic strain field related to the compositional modulation phenomenon^{8–14} should determine the InP dot nucleation positions on the surface of InGaP layer. Moreover, no significant effect on dot shape and size has been observed due to the presence of this strain field.

All samples were grown by chemical-beam epitaxy (CBE) on semi-insulating (001) GaAs substrates. Details of the growth conditions are provided elsewhere.⁵ A 300 nm GaAs film was grown as a buffer layer at 550 °C and growth

rate of 0.72 $\mu\text{m}/\text{h}$ followed by a 450 nm thick InGaP layer. On top of the InGaP layer, 4 monolayers (MLs) of InP at a growth rate of 0.2 ML/s and 540 °C were deposited. The V/III ratio during InGaP growth was 17 for Samples A and B, and 32 for Sample C, discussed here. Such a V/III ratio variation was obtained by changing the PH_3 flux only. The InGaP layers of Samples A, B, and C were grown at 550 °C at a growth rate of 0.95 $\mu\text{m}/\text{h}$. These samples are similar to Samples 3, 4, and 6 discussed in Ref. 5. In order to perform plan-view TEM and AFM measurements, additional samples without InP on top of the InGaP layer were grown at the same conditions used for samples with InP dots.

The reflection high-energy electron diffraction (RHEED) patterns were monitored during the growth process; the InGaP surface shows a (2×1) reconstruction for all samples. Plan-view and cross-sectional images were obtained using a JEM 3010 URP 300-kV TEM. AFM images were performed in air operating in noncontact mode and using conical silicon tips. The lattice mismatch ($\Delta a/a$) between InGaP and GaAs was <0.05 , 0.60, and 0.66, respectively, for Samples A, B, and C. Such values were obtained from (004) rocking curves using double-crystal x-ray diffractometry (XRD). The TEM studies indicate that all samples are dislocation free.

Figure 1 shows cross-sectional $g=(220)$ dark-field TEM images from Samples A, B, and C. In this mode, dark/bright contrasts are mainly caused by lattice distortions on crystal-line planes. In epitaxial films, such distortions are generally originated by strain misfit variations inside the layer. For ternary or quaternary alloys, several works have shown that the presence of periodic distortions perpendicular to the growth direction is related to compositional modulation.^{7–10} This phenomenon consists of the spontaneous periodic variation of alloy composition along the layer. Such compositional variations depend strongly on the growth conditions and have been extensively investigated in the last years.^{10–14}

Figure 1 shows that the dark/bright contrasts are indeed present in our samples. Figure 1(a) shows a weak contrast near the GaAs interface for Sample A, with no clear period observed along the layer. This result indicates that the lattice-matched InGaP layer (grown at 550 °C and V/III ratio equal to 17) is rather homogeneous. On the other hand, Sample B [Fig. 1(b)] presents a strong periodic dark/bright contrast along the $[110]$ direction. This difference between Samples

^{a)}Electronic mail: jrborto@ifi.unicamp.br

^{b)}Present address: Penn State University, Department of Physics, Institute of Materials Science, University Park, Pa 16802.

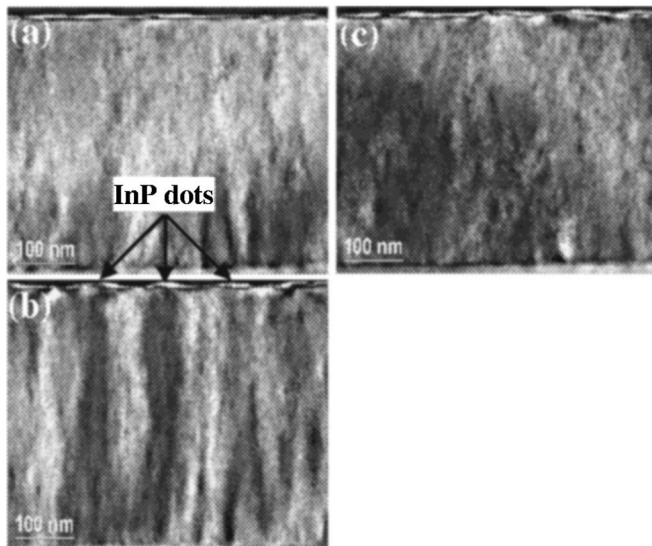


FIG. 1. Cross-sectional $g=(220)$ dark-field TEM images of the InP/InGaP samples grown at temperature of 550 °C and V/III ratio of (a) 17, (b) 17, and (c) 32. The periodic dark/bright contrast on Sample B is associated with the compositional variation on InGaP layer. The InP dots are mainly positioned on top of dark regions on Sample B.

A and B is most likely associated with the strain misfit due to the 0.6% mismatch in the InGaP layer; the induced compositional modulation gives rise to periodic dark/bright contrasts perpendicular to the growth direction. Figure 1(c) shows the TEM image for Sample C, grown at same conditions used for Sample B except for the V/III ratio (about 32 to Sample C). The rather homogeneous contrast seen in Fig. 1(c) suggests that the compositional modulation phenomenon in our set of samples also depends on the V/III ratio. In this case, one can assume that surface mechanisms play an important role on compositional modulation phenomenon for InGaP grown by CBE.

Although many theoretical works^{10–14} predict morphological instabilities coupled to compositional segregation phenomenon, our AFM data show that the InGaP surface remains basically smooth, even for thick samples; the root-mean-square roughness values on $3\ \mu\text{m} \times 3\ \mu\text{m}$ area are 0.39 nm, 0.20 nm, and 0.38 nm for films grown at the same conditions as for Samples A, B, and C, respectively.

The cross-sectional TEM image from Fig. 1(b) alone cannot point out if the compositional modulation is really along the $[110]$ direction or along one $\langle 100 \rangle$ direction. Furthermore, some experimental reports^{6,7} have shown a two-dimensional pattern of compositional variations. For example, Henoc *et al.*⁶ reported that the compositional modulation in InGaAsP grown on an InP substrate by liquid phase epitaxy exhibits a two-dimensional pattern with period about 100 nm.⁶ For this reason, we have performed plan-view measurements of a sample grown under the same conditions used for Sample B, but with no InP grown on top of the InGaP buffer layer. The bright-field TEM image is seen in Fig. 2. We can observe a clear two-dimensional array of brighter regions roughly aligned at $[100]$ and $[010]$ directions. Hence, the periodic dark/bright pattern shown in Fig. 1(b) is a projection of the two-dimensional compositional modulation.

Energy dispersive x-ray measurements, taken during the plan-view imaging (with lateral resolution of 20 nm) on this same sample, show that the InGaP layer presents an alloy

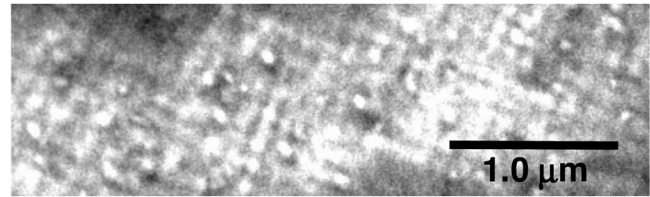


FIG. 2. Plan-view TEM image of InGaP layer grown at the same conditions used for Sample B.

composition varying from $\text{In}_{0.542}\text{Ga}_{0.458}\text{P}$ to $\text{In}_{0.590}\text{Ga}_{0.410}\text{P}$. This result is an independent confirmation of compositional modulation phenomenon in Sample B.

The competition between thermodynamic and kinetic effects can give rise to metastable bulk properties^{10–15} during growth of alloy films. In particular, InGaP layers usually also exhibit CuPt_B atomic ordering¹⁵ further than compositional modulation.^{6–11} Indeed, photoluminescence measurements reported in our previous work⁵ showed the presence of CuPt -type-ordered domains inside the InGaP layers. In order to investigate their spatial distribution and size, we have also performed $[110]$ cross-sectional dark-field images taken with $(\frac{1}{2}, \frac{1}{2}, \frac{1}{2})$ excitation. In this condition, the bright regions in the TEM image are CuPt -type ordered domains. Our results show that all three samples present these domains randomly distributed in the InGaP buffer. Moreover, Sample C presents the larger-ordered phase volume (domains up to 20 nm in size) while for Samples A and B atomic ordering is almost absent (size of domains up to 5 nm). In agreement with previous works¹⁵ and our photoluminescence results,⁵ the ordered phase volume increases with P_2 overpressure.

From the point of view of InP/InGaP growth, any local changes in the structural properties of the InGaP layer can lead to preferential nucleation sites for InP self-assembled islands. In this way, our experimental measurements show a clear correlation between InP dot position and the compositional modulation phenomenon. In contrast, no correlation is observed with the atomic ordering phenomenon. This assumption is essentially supported by our observations. First, the AFM analysis shows that the InP dots are randomly distributed on Samples A and C, although on Sample B they are spatially organized in a two-dimensional array—for the same InP growth conditions. On the other hand, compositional modulation is observed only for the InGaP layer of Sample B, while CuPt -type-ordered domains are randomly distributed inside the InGaP layer for all three samples. Regarding the lateral ordering, InP dots on Sample B are roughly aligned to the $[100]$ and $[010]$ directions, similar to the array displayed by InGaP brighter regions in Fig. 2. Also, the period of both dot array and compositional modulation is about 100 nm. Finally, we can note from Fig. 1(b) that the InP dots are indeed mainly positioned on top of the dark regions.

The periodic variation of InGaP composition must interact with the dot nucleation via their elastic strain field. Because of the lattice distortion in the InGaP layer, the strain distribution on the InP wetting layer is given by the superposition of the homogeneous lattice-mismatch strain and the contribution of the smaller but periodic strain field created by the compositional modulation. The effect is qualitatively similar to that created by buried InP dots on the surface of a cap $\text{In}_{0.485}\text{Ga}_{0.515}\text{P}$ layer (mismatch $\varepsilon_0 \sim 3.8\%$). In order to make a quantitative evaluation of this hypothesis, we have

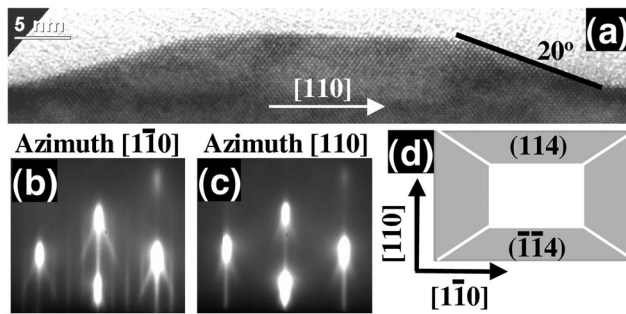


FIG. 3. (a) Cross-sectional $[1\bar{1}0]$ high-resolution TEM of a typical InP dot from Sample B, showing a flat top and sidewalls with angle $\sim 20^\circ$. (b) RHEED pattern showing 2×4 reconstruction and chevrons that indicate facet formation. (c) No chevrons are seen at this direction. (d) Schematic representation of InP shape deduced from TEM, RHEED, and AFM data.

estimated the strain associated to $\text{In}_{0.590}\text{Ga}_{0.410}\text{P}$ (lattice parameter $d=5.6972 \text{ \AA}$) columnlike clusters inside a $\text{In}_{0.542}\text{Ga}_{0.458}\text{P}$ ($d=5.6771 \text{ \AA}$) matrix ($\varepsilon_0 \sim 0.35\%$). We thus used the pointlike source approximation and integrated on volume¹⁶ for two cases: Cylindrical buried InP islands with 35 nm radius and 5 nm height and In-rich columns with the same radius but 450 nm high for the modulated InGaP. The calculation shows that the strain on InGaP surface in this latter case is equivalent to that created by buried InP islands with a 18 nm thick spacer. These values should allow the vertical correlation of dots according to experimental observations.¹⁷

In spite of the lateral positioning, our results show that the strain field related to compositional modulation alters neither the shape nor the density of InP dots. Figure 3(a) exhibits a cross-sectional $[110]$ high-resolution TEM (HRTEM) of a typical InP dot from Sample B. We can observe that this island is surrounded by a flat top and two lateral planes with 20° inclination angle. This angle is well-matched to $\{114\}$ crystallographic facets. On the other hand, cross-sectional $[110]$ HRTEM (not shown) of Sample B shows InP islands delimited by a (001) plane on top but with no particular angle on the lateral sides.

In statistical terms, the appearance of chevrons in the RHEED pattern shown in Fig. 3(b) indicates that the majority of InP islands of Sample B is actually formed by (114) and $[\bar{1}\bar{1}4]$ planes. Moreover, the absence of such chevrons in the $[110]$ azimuth [Fig. 3(c)] corroborates the HRTEM results. The further analysis of the RHEED pattern during InP nucleation indicates the same evolution for all samples discussed here, independent of the lateral dot ordering degree.

The *ex situ* AFM measurements are in agreement with HRTEM and RHEED results mentioned above. In addition, the AFM results show that the InP dots are slightly elongated at the $[1\bar{1}0]$ crystallographic direction. Through these data, we assume that the stable InP shape is an elongated truncated pyramid as schematically shown in Fig. 3(d). The sides more stretched out are formed by $\{114\}$ facets and the top is shaped by (001) plane. These characteristics are essentially the same for all samples presented here.

The statistical analysis of $1.5 \mu\text{m} \times 1.5 \mu\text{m}$ AFM images show that the island density is about $1.5 \times 10^{10} \text{ cm}^{-2}$ for

Sample B. The average height and radius are $5.2 \pm 1.5 \text{ nm}$ and $35 \pm 7 \text{ nm}$, respectively. Again, other samples exhibit similar results. For example, the island height and radius for Sample A are $5.0 \pm 1.4 \text{ nm}$ and $33 \pm 6 \text{ nm}$, respectively.

With regard to the optical properties of InP dots, photoluminescence measurements indicate that they are also unchanged by the lateral dot alignment. In particular, the photoluminescence peak of dot emission for Sample B is around 1.697 eV and exhibits a linewidth of 54 meV. For Sample A, the peak is redshifted only 9 meV with the same linewidth. These results altogether show that either shape, size, and optical properties remain basically the same regardless of the presence of the periodic strain field in the InGaP layer.

In summary, our work shows that the compositional modulation in the InGaP layer creates preferential sites to InP dot nucleation via the related periodic strain field. The compositional variation is along $[100]$ and $[010]$ crystallographic directions. The periodic dark/bright pattern observed in cross section TEM is a projection of this two-dimensional compositional modulation. The presence of this phenomenon and, consequently, the spatial ordering of InP dots are dependent on the growth conditions, including P_2 overpressure. Although the periodic strain field in the InGaP buffer from Sample B is large enough to align the InP dots, both their shape and optical properties are effectively unaltered.

This work was supported by the Brazilian Agencies FAPESP, CNPq, and FINEP. Two of the authors (J.R.R.B. and H.R.G.) acknowledge financial support from FAPESP. The TEM measurements were made at the LME facilities of the National Laboratory of Synchrotron Light (LNLS), Brazil. The authors also thank Dr. L. P. Cardoso and R. Marcon for technical assistance with the XRD measurements.

¹For a review, see, for example, L. Jacak, P. Hawrylak, and A. Wojs, *Quantum Dots* (Springer, Berlin, 1998).

²For a review, see, for example, V. Shchukin, and D. Bimberg, *Rev. Mod. Phys.* **71**, 1125 (1999).

³H. Lee, J. A. Johnson, M. Y. He, J. S. Speck, and P. M. Petroff, *Appl. Phys. Lett.* **78**, 105 (2001).

⁴C.-S. Lee, B. Kahng, and A.-L. Barabási, *Appl. Phys. Lett.* **78**, 984 (2001).

⁵J. R. R. Bortoleto, H. R. Gutiérrez, M. A. Cotta, J. Bettini, L. P. Cardoso, and M. M. G. de Carvalho, *Appl. Phys. Lett.* **82**, 3523 (2003).

⁶P. Henoc, A. Izrael, M. Quilec, and H. Launois, *Appl. Phys. Lett.* **40**, 963 (1982).

⁷R. R. LaPierre, T. Okada, B. J. Robinson, D. A. Thompson, and G. C. Weatherly, *J. Cryst. Growth* **155**, 1 (1995).

⁸F. Peiró, A. Cornet, J. R. Morante, A. Georgakilas, C. Wood, and A. Christou, *Appl. Phys. Lett.* **66**, 2391 (1995).

⁹T. Okada, G. C. Weatherly, and D. W. McComb, *J. Appl. Phys.* **81**, 2185 (1997).

¹⁰J. E. Guyer, S. A. Barnett, and P. W. Voorhees, *J. Cryst. Growth* **217**, 1 (2000).

¹¹F. Léonard and R. C. Desai, *Appl. Phys. Lett.* **74**, 40 (1999).

¹²Z.-F. Huang and R. C. Desai, *Phys. Rev. B* **65**, 205419 (2002).

¹³B. J. Spencer, P. W. Voorhees, and J. Tersoff, *Appl. Phys. Lett.* **76**, 3022 (2000).

¹⁴B. J. Spencer, P. W. Voorhees, and J. Tersoff, *Phys. Rev. B* **64**, 235318 (2001).

¹⁵A. Zunger, *Mater. Res. Bull.* **22**, 20 (1997); G. B. Stringfellow, *ibid.* **22**, 27 (1997).

¹⁶J. Zhang, K. Zhang, and J. Zhonga, *Appl. Phys. Lett.* **84**, 1853 (2004).

¹⁷M. K. Zundel, P. Specht, K. Eberl, N. Y. Jin-Phillip, and F. Phillip, *Appl. Phys. Lett.* **71**, 2972 (1997).